



**HAL**  
open science

# Connectivity networks and delineation of disconnected coastal provinces along the Indian coastline using large-scale Lagrangian transport simulations

D. Bharti, Katell Guizien, M. Aswathi-das, P. Vinayachandran, Kartik Shanker

## ► To cite this version:

D. Bharti, Katell Guizien, M. Aswathi-das, P. Vinayachandran, Kartik Shanker. Connectivity networks and delineation of disconnected coastal provinces along the Indian coastline using large-scale Lagrangian transport simulations. 2022. hal-03209597v1

**HAL Id: hal-03209597**

**<https://hal.science/hal-03209597v1>**

Preprint submitted on 16 May 2022 (v1), last revised 13 Dec 2022 (v2)

**HAL** is a multi-disciplinary open access archive for the deposit and dissemination of scientific research documents, whether they are published or not. The documents may come from teaching and research institutions in France or abroad, or from public or private research centers.

L'archive ouverte pluridisciplinaire **HAL**, est destinée au dépôt et à la diffusion de documents scientifiques de niveau recherche, publiés ou non, émanant des établissements d'enseignement et de recherche français ou étrangers, des laboratoires publics ou privés.

1 **Title:**

2 Connectivity networks and delineation of disconnected coastal provinces along the Indian  
3 coastline using large-scale Lagrangian transport simulations

4

5 **Running Title:**

6 Lagrangian simulations of connectivity along the Indian coastline

7

8 **Authors:**

9 D. K. Bharti<sup>1,2\*</sup> (ORCID ID: 0000-0002-5657-6952), Katell Guizien<sup>3</sup> (ORCID ID: 0000-0001-  
10 9884-7506), M. T. Aswathi-Das<sup>4,5</sup> (ORCID ID: 0000-0002-8857-2294), P. N.  
11 Vinayachandran<sup>5</sup> (ORCID ID: 0000-0002-4915-5455) and Kartik Shanker<sup>1</sup> (ORCID ID: 0000-  
12 0003-4856-0093)

14 **Affiliations:**

15 <sup>1</sup> Centre for Ecological Sciences, Indian Institute of Science, Bengaluru, India

16 <sup>2</sup> CSIR-Centre for Cellular and Molecular Biology, Hyderabad, India

17 <sup>3</sup> CNRS, Sorbonne Université, Laboratoire d'Ecogéochimie des Environnements Benthiques  
18 (LECOB), Observatoire Océanologique de Banyuls, Banyuls-sur-Mer, France

19 <sup>4</sup> National Centre for Polar and Ocean Research, Ministry of Earth Sciences, Goa, India

20 <sup>5</sup> Centre for Atmospheric and Oceanic Sciences, Indian Institute of Science, Bengaluru, India

21

22 **\*Corresponding author:**

23 Address: Dr. D. K. Bharti, c/o Dr. Jahnavi Joshi, CSIR-Centre for Cellular and Molecular  
24 Biology, Uppal Road, Habsiguda, Hyderabad – 500 007, India

25 Email: [bhartidk@csircmb.org](mailto:bhartidk@csircmb.org)

## 26 **Abstract**

27

28 Ocean circulation is the engine of dispersal and population connectivity in marine  
29 ecosystems, knowledge of which is essential for conservation planning. Understanding  
30 connectivity patterns at a large scale can help define the spatial extent of metapopulations. In  
31 this study, we built connectivity networks from Lagrangian transport simulations of neutrally  
32 buoyant particles, released along the Indian coastline, a significant region in the Indian  
33 Ocean. We assessed the variation in connectivity networks across release periods for the  
34 major drivers of oceanography including the two monsoonal seasons, El Niño–Southern  
35 Oscillation (ENSO) years and for the entire range of region-specific pelagic larval durations  
36 (PLD) for marine invertebrates. We detected well-connected communities, mapped frequent  
37 connectivity breaks and assessed the functional role of coastal areas within the connectivity  
38 network using node metrics. Network characteristics did not differ based on the ENSO year,  
39 but varied with season and PLD. [Connectance for the Indian coastline was relatively low,](#)  
40 [ranging from 0.5% to 3.4%, and increased significantly for PLD larger than 20 days.](#) The  
41 number of cohesive coastal communities decreased gradually from 60 (PLD <4 days) to 30  
42 (PLD >20 days) with increasing PLD. Despite variation in the location of connectivity breaks  
43 with the time of particle release within a monsoonal season, four disconnected provinces  
44 were consistently identified across the entire PLD range, which partially overlapped with  
45 observed genetic and biogeographic breaks reported along the Indian coastline. Our results  
46 support the adoption of coordinated management framework within each of the four  
47 provinces delineated in the present study.

48

49 **Keywords:** biophysical model, dispersal, connectivity, Indian Ocean, marine biogeography

## 50 **Introduction**

51

52 Marine populations have traditionally been described as ‘open’, with high exchange of  
53 propagules between spatially distant populations owing to oceanic transport of pelagic life  
54 stages (Roughgarden et al., 1988). However, it is the interaction between oceanographic  
55 features, habitat distribution and species-specific traits that determines if a population falls in  
56 the continuum from ‘open’ to ‘closed’, within a meta-population framework (Levin, 2006).  
57 Biophysical modelling, which combines ocean circulation simulations with larval traits and  
58 habitat information, is a useful tool to explore patterns of larval transport in the ocean  
59 (Swearer et al., 2019). Ocean flow and pelagic larval duration (PLD) are the minimum  
60 parameters required to assess seascape connectivity (North et al., 2009), though biological  
61 parameters related to larval behaviour can strongly influence dispersal patterns (Robins et al.,  
62 2013).

63

64 Biophysical simulations of larval transport based on coarse-resolution global ocean  
65 circulation simulations can serve as a foundation for regional ecological studies by  
66 delineating large-scale disruptions in connectivity (Jacobi et al. 2012; Rossi et al., 2014).  
67 Identifying the extent of well-connected regions, within which spatially distinct populations  
68 exchange individuals to give rise to a metapopulation (Hanski & Gaggiotti, 2004), is essential  
69 for coordinating biodiversity management (Halpern & Warner, 2003; Mertens et al. 2018).  
70 This is especially important for tropical continental coastlines, which have received less  
71 attention in marine ecology studies (Partelow et al., 2018). Since management policies are a  
72 national prerogative, it is also important to include all the regions falling within the  
73 boundaries of marine resource governance. Identifying the extent and strength of connectivity

74 spanning regional and national boundaries can help in focusing conservation efforts leading  
75 to more effective management (Treml & Halpin, 2012).

76

77 The Exclusive Economic Zone (EEZ) of India includes (1) a coastline of over 5400 km that  
78 divides the northern Indian Ocean into two basins – the Arabian Sea in the west and the Bay  
79 of Bengal in the east, (2) the Lakshadweep archipelago located in the Arabian Sea, and (3) the  
80 Andaman and Nicobar archipelago located in the Bay of Bengal. Sri Lanka is an island  
81 located in the Bay of Bengal, which is separated from India by the narrow Palk Strait, where  
82 both countries have contiguous EEZs (Figure 1). There is an absence of large-scale  
83 connectivity studies from the northern Indian Ocean (see George et al., 2011 and Gaonkar et  
84 al., 2012 for local-scale studies) despite a large body of physical oceanography research from  
85 this region (reviewed in Schott et al., 2009).

86

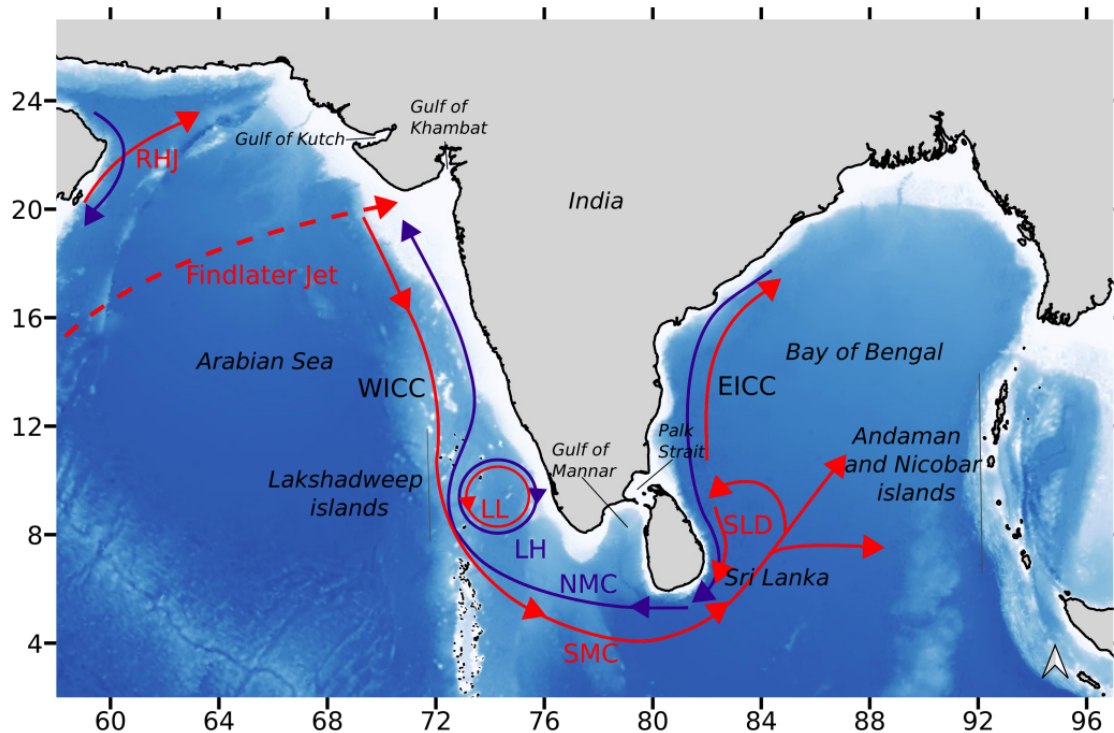
87 The upper ocean circulation along the coasts of India is driven by seasonally reversing  
88 monsoon winds (Schott & McCreary, 2001). During the summer (south-west) monsoon from  
89 June to September, the West India Coastal Current (WICC) flows towards the equator along  
90 the west coast of India (Shetye & Gouveia, 1998, Amol et al., 2014) and merges with the  
91 South-West Monsoon Current (SMC). It turns around the southern tip of India bringing saltier  
92 water into the Bay of Bengal, and joins the northern branch of the Sri Lanka Dome  
93 (Vinayachandran & Yamagata, 1998) flowing poleward as the East India Coastal Current  
94 (EICC) (Mukherjee et al., 2014) (Figure 1). During this period, coastal upwelling events of  
95 varying intensity occur along the west coast of India (Luis & Kawamura, 2004; Hood et al.,  
96 2017), with weak upwelling along the eastern coast of India, and the Andaman and Nicobar  
97 islands (Varkey et al. 1996; Vinayachandran et al., 2021).

98

99 During the winter (north-east) monsoon from November to February, the circulation along  
100 the east coast of India reverses direction to flow equatorward (EICC) (Shetye & Gouveia,  
101 1998, Mukherjee et al., 2014), turns around the southern tip of India (Winter Monsoon  
102 Current) and flows poleward along the west coast (WICC), bringing fresher water into the  
103 Arabian Sea (Figure 1, Shetye & Gouveia, 1998; Amol et al., 2014). Together with  
104 alongshore flow reversal, upwelling reverses into downwelling events within a 40 km wide  
105 band along the east coast of India (Varkey et al. 1996) and along the north-west coast of India  
106 (Luis & Kawamura, 2004).

107

108 The seasonal wind-driven circulation described above is modulated at several time-scales  
109 (Schott et al. 2009) ranging from intra-seasonal to inter-annual variation. Intra-seasonal  
110 atmospheric oscillations act at time-scales ranging from a week (northward propagating  
111 precipitation anomalies) to 30-60 days (Madden-Julian Oscillation, Madden & Julian 1972).  
112 Inter-seasonal variation in circulation arises from both El Niño Southern Oscillation, leading  
113 to a year-long basin-scale warming after El Niño events, and Indian Ocean Dipole events,  
114 with cool (warm) and dry (wet) anomalies in the eastern (western) Indian Ocean  
115 (Vinayachandran et al. 2009). In such a complex oceanographic context with large to meso-  
116 scale structures, it is difficult to a priori anticipate how biological filters such as the time of  
117 larval release and PLD might shape connectivity along the vast Indian coastline.



118

119 **Figure 1.** Schematic illustration of major currents along the Indian coastline. From west to  
 120 east – Ras al Hadd Jet (RHJ), West India Coastal Current (WICC), Lakshadweep Low (LL),  
 121 Lakshadweep High (LH), South-West Monsoon Current (SMC), North-East Monsoon  
 122 Current (NMC), SLD (Sri Lanka Dome) and East India Coastal Current (EICC). Findlater Jet  
 123 is an atmospheric jet observed in the northern Arabian Sea during the summer monsoon.  
 124 Processes associated with the summer monsoon are in red and those associated with the  
 125 winter monsoon are in blue. WICC and EICC occur in both monsoons but differ in direction  
 126 as indicated by the coloured arrows.

127 In the current study, we aim to describe patterns of oceanographic connectivity along the  
128 Indian coastline. To do so, we carried out Lagrangian transport simulations of neutrally  
129 buoyant particles released along the coastline during the two major seasons – summer and  
130 winter monsoon, for three years and across a wide range of PLD. Transport simulations were  
131 post-processed to build coastal connectivity networks for different combinations of season,  
132 year and PLD. The specific aims of our study were to (1) identify breaks in oceanographic  
133 connectivity and analyze their stability across years, seasons and PLD, and (2) examine the  
134 implications of these connectivity breaks for biodiversity management.

135

## 136 **Materials**

137

### 138 *Ocean circulation data*

139

140 We used HYCOM (Chassignet et al., 2007) global ocean circulation reanalysis data  
141 (<https://www.hycom.org/dataserver/gofs-3pt0/reanalysis>) for running particle tracking  
142 simulations. HYCOM reproduces the main circulation features around the Indian peninsula  
143 (Supplementary Information 1), and simulations at various resolutions have validated its  
144 application in operational oceanography (George et al. 2010, Joseph et al. 2018). We acquired  
145 HYCOM output at 0.08° horizontal spatial resolution, 40 z-levels in depth and 3-hour  
146 temporal frequency for the spatial extent ~30°N-10°S, 50°W-100°E and the years 2008-2011.  
147 This temporal range captures the variation in ocean circulation presented by various states of  
148 the El Niño–Southern Oscillation (ENSO), as 2009-2010 represents an El Niño year, while  
149 2011 was a La Niña year ([https://psl.noaa.gov/enso/past\\_events.html](https://psl.noaa.gov/enso/past_events.html)). Particle transport in  
150 the vertical, which is particularly important in coastal areas with upwelling or downwelling,

151 was accounted for after reconstructing vertical velocity values (not available in the HYCOM  
152 repository) using the continuity equation of mass conservation. This was done for the upper  
153 27 depth levels from surface, i.e. down to 400 m deep, to avoid anomalies that can arise in  
154 reconstruction at further depths.

155

#### 156 *Particle tracking procedure*

157

158 We ran three-dimensional neutrally buoyant particle tracking simulations with the  
159 Connectivity Modeling System (Paris et al., 2013). Particles were released along the Indian  
160 subcontinent, Sri Lanka, Lakshadweep islands and the Andaman and Nicobar islands. Release  
161 locations were placed at a distance of 12 km from the coastline to avoid unresolved flow  
162 velocities at the coast and to ensure at least 3 vertical levels of ocean flow input (bathymetry  
163 ranging from 4 m to 2500 m, Supplementary Information 2). Particles were released 1 m  
164 below the surface, every 5 km along the coastline (2136 release locations) during the summer  
165 (June to September) and the winter (November to February) monsoons, in release periods  
166 spanning ten days each. Successive particle positions were calculated using a time-step of 20  
167 minutes and recorded every three hours, for over six million particles in each season.  
168 Particles were tracked for a period of 50 days, informed by the distribution of PLD for marine  
169 invertebrates found in this region (Supplementary Information 3).

170

171 In the present study, we chose to scan a wide range of species by varying dispersal duration  
172 and release timing to model large-scale connectivity that is generalizable across taxa. Our use  
173 of neutrally buoyant particles assumes limited larval behaviour and does not capture the

174 effect of species-specific variation in larval motility (e.g. nyctemeral vertical migration),  
175 which can influence connectivity estimates between species.

176

177 *Connectivity networks*

178

179 The coastal area was divided into 528 coastal polygons,  $\sim 200 \text{ km}^2$  in area, overlaid over  
180 particle release locations (Supplementary Information 4). Connectivity matrices of particle  
181 transfer (278,784 possible connections) were built by calculating the proportion of particles  
182 released in a source coastal polygon that successfully dispersed to a destination coastal  
183 polygon. Particle transfer per unit surface was obtained by scaling particle transfer values  
184 with the the area of the destination polygon. [This was done to correct for the differences in](#)  
185 [area between destination polygons, which can influence the probability of a particle reaching](#)  
186 [it](#) (Fig 2). Instead of using a representative subset of PLDs, and to make our results  
187 generalizable across all possible dispersal durations, we analyzed connectivity matrices  
188 across PLDs ranging between 2 to 50 days, with an interval of 2 days. Based on the  
189 frequency distribution of PLDs for marine invertebrates collated for the Indian Ocean  
190 (Supplementary Information 3), connectivity matrices were averaged into four PLD-classes  
191 for each release period – 2-4 days, 6-12 days, 14-20 days and 22-50 days (4 PLD-classes  $\times$  2  
192 seasons  $\times$  12 release periods  $\times$  3 years = 288 connectivity matrices).

193

194 Each connectivity matrix defined a directed weighted graph (called connectivity network  
195 hereafter), where nodes were coastal polygons and directed weighted edges between each  
196 pair of source and destination nodes were values of particle transfer per unit surface between  
197 them (Figure 2). Various metrics were used to describe the connectivity network.

198 Connectance is a global property of a network, which measures the overall network density  
199 (number of realized connections in comparison with all possible connections), and is  
200 calculated as the proportion of non-zero edges within a network. The number of singleton  
201 nodes is the count of isolated nodes (with no connection), which indicates the extent of the  
202 network. To further understand the structure of the network density indicated by connectance,  
203 we identified and counted two kinds of network components. A weak subgraph consists of  
204 nodes that are connected to each other irrespective of direction and indicates weak  
205 connectivity between nodes. On the other hand, a strong subgraph is more well-connected  
206 network component where each pair of nodes is connected in both directions, and reflects  
207 strong bidirectional connectivity.

208

209 Particle release locations and coastal polygons were created using the packages ‘*raster*’  
210 (Hijmans, 2020), ‘*rgeos*’ (Bivand & Rundel, 2020), ‘*sp*’ (Pebesma & Bivand, 2005; Bivand et  
211 al., 2013) in R version 3.6.1 (R Core Team, 2019), and further edited in QGIS 3.14.0-Pi  
212 (QGIS.org, 2021).

213

214 *Community detection*

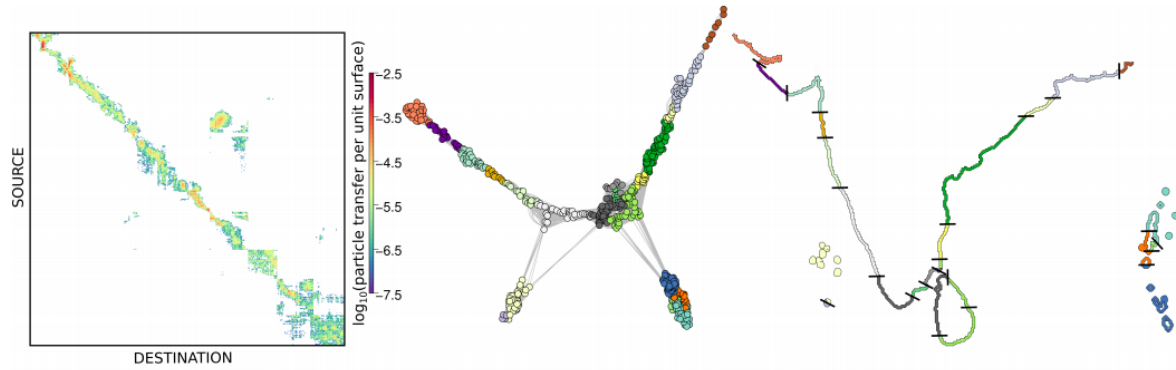
215

216 Each connectivity network was individually processed to detect communities using the  
217 Infomap algorithm (Rosvall & Bergstrom, 2008) (Figure 2) by applying the  
218 ‘*cluster\_infomap*’ function in the ‘*igraph*’ package (Csardi & Nepusz, 2006) in R version  
219 3.6.1 (R Core Team, 2019). This algorithm uses information-theoretic principles to define a  
220 community based on the ease of flow between nodes of a directed weighted network. A  
221 community is detected when a random walker visits a set of nodes within the network more

222 often than nodes outside it and is likely to get trapped between them (Rosvall & Bergstrom,  
223 2008).

224

225 The significance of a detected community was estimated using its coherence ratio – the  
226 proportion of particles that originate from nodes within a community and remain within the  
227 same community (Rossi et al., 2014). A coherence ratio greater than 0.5 was applied to detect  
228 well connected communities, and the location of community boundaries (referred to as  
229 community breaks henceforth) was identified. Community breaks were classified based on  
230 their frequency of occurrence across release periods within a PLD-class. Those occurring with  
231 a frequency greater than 50% were termed ‘frequent’ and those with a frequency greater than  
232 90% were termed ‘persistent’. Persistent community breaks were used to identify  
233 connectivity provinces along the Indian coastline. Connectivity between island groups and  
234 connectivity provinces was evaluated by analyzing their co-occurrence in detected  
235 communities using the Bray-Curtis similarity measure, while accounting for variation in the  
236 number of coastal polygons between regions (Baselga, 2017) using the ‘*betapart*’ package  
237 (Baselga & Orme, 2012) in R version 3.6.1 (R Core Team, 2019).



238

239 **Figure 2.** Schematic figure depicting the various stages in connectivity analysis, which  
 240 include (left) connectivity matrix obtained from particle trajectories, (center) connectivity  
 241 network with nodes coloured based on Infomap communities and (right) connectivity breaks  
 242 derived from Infomap community boundaries. The figures shown here are derived from a  
 243 mean connectivity matrix across release periods and years for the PLD-class 14-20 days  
 244 during the summer monsoon.

245 *Statistical tests*

246

247 The significance of the variation in the distributions of connectance, the number of singleton  
248 nodes, weak and strong subgraphs and Infomap communities with >1 membership, with  
249 PLD-class, year and season was evaluated using non-parametric Kolmogorov-Smirnov test in  
250 R version 3.6.1 (R Core Team, 2019).

251

252 *Nodes descriptors*

253

254 Apart from network-level metrics, we also calculated node-level metrics of connectivity to  
255 understand the variation in the number of connections (degree) and flux intensity of  
256 connections (strength) to or from a node (coastal polygon). The total node degree and  
257 strength can be used to compare the contribution of different nodes to the overall connectivity  
258 in a network. Proportion in-degree is the relative magnitude of incoming connections with  
259 respect to total connections at a node, and indicates its influence in comparison to other nodes  
260 in the network. High in-degree indicates a node under the influence of other nodes, while low  
261 in-degree indicates that the node influences other nodes in the network. Proportion of in-  
262 strength indicates the relative magnitude of import with respect to total traffic through a node,  
263 and can be associated with its role as a source or a sink location. These measures were  
264 calculated using functions implemented in R version 3.6.1 (R Core Team, 2019).

265

266 **Results**

267

268 There was no significant variation in most connectivity network characteristics between  
269 years, while their variation between release periods within a year was large (Supplementary  
270 Information 5). Based on these results, variability of all the network metrics was estimated  
271 after pooling 36 connectivity matrices across 12 release periods for each PLD-class and  
272 season across three years.

273

274 *Network descriptors*

275

276 Connectance ranged from 0.5% to 3.4% across PLD-class and season, and showed the  
277 greatest significant difference between PLD less than 20 days and PLD greater than 20 days  
278 in both seasons (Figure 3). A significant increase in connectance indicates that a PLD of 20  
279 days is pivotal to ensure significant transport farther than 2-5 km (range of shortest distance  
280 between a release location and adjacent coastal polygon) along the coastline.

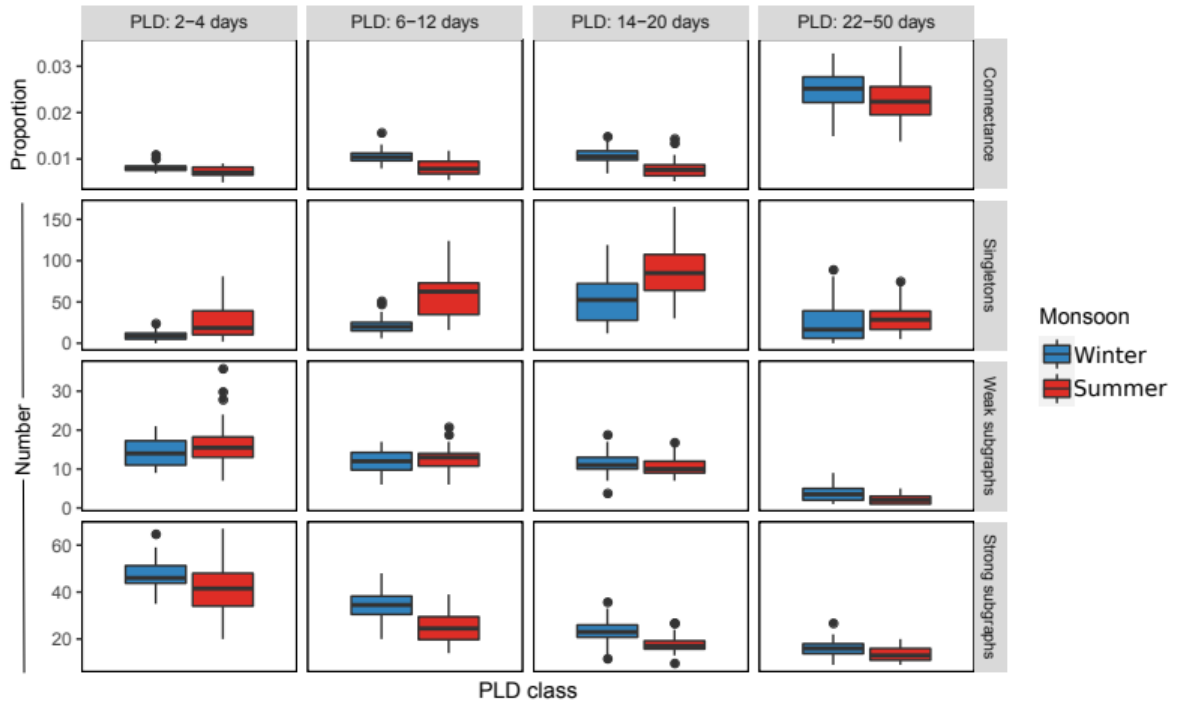
281

282 There were less than 30% disconnected singleton nodes across PLD-classes and seasons  
283 (Figure 3). The number of singleton nodes increased till a PLD of 20 days (Supplementary  
284 Material 5), indicating that local connections with neighbouring coastal polygons seen at  
285 shorter PLDs disappeared as particles dispersed away from the coast at intermediate PLDs.

286

287 The number of weak subgraphs largely remained unchanged for PLD less than 20 days (4-  
288 36), while the number of strong subgraphs significantly decreased between the PLD less than  
289 6 days (20-67) and the PLD greater than 20 days (9-27) (Supplementary Material 5). This  
290 indicates that there was an increase in the number of bi-directional connections within  
291 subgraphs with increasing PLD. This densification of subgraphs, for PLD up to 20 days, was

292 more pronounced in the summer monsoon as compared to the winter monsoon  
293 (Supplementary Information 5).



294

295 **Figure 3.** Summary characteristics of connectivity networks.

296 *Infomap communities*

297

298 Similar to the trend observed with strong subgraphs, the number of Infomap communities  
299 (communities hereafter) decreased with an increase in PLD (Figure 4a). Except for the PLD-  
300 class 6-12 days, the number of communities detected for the same PLD-class was not  
301 significantly different between seasons (Supplementary Material 5). The coherence ratio of  
302 the detected communities showed little variation for PLD classes less than 20 days, but  
303 showed the greatest variability for PLD larger than 20 days and during the summer monsoon  
304 (Supplementary Material 5) (Figure 4b). The decrease in coherence ratio indicates a decrease  
305 in the exchange of particles within a community through losses outside it.

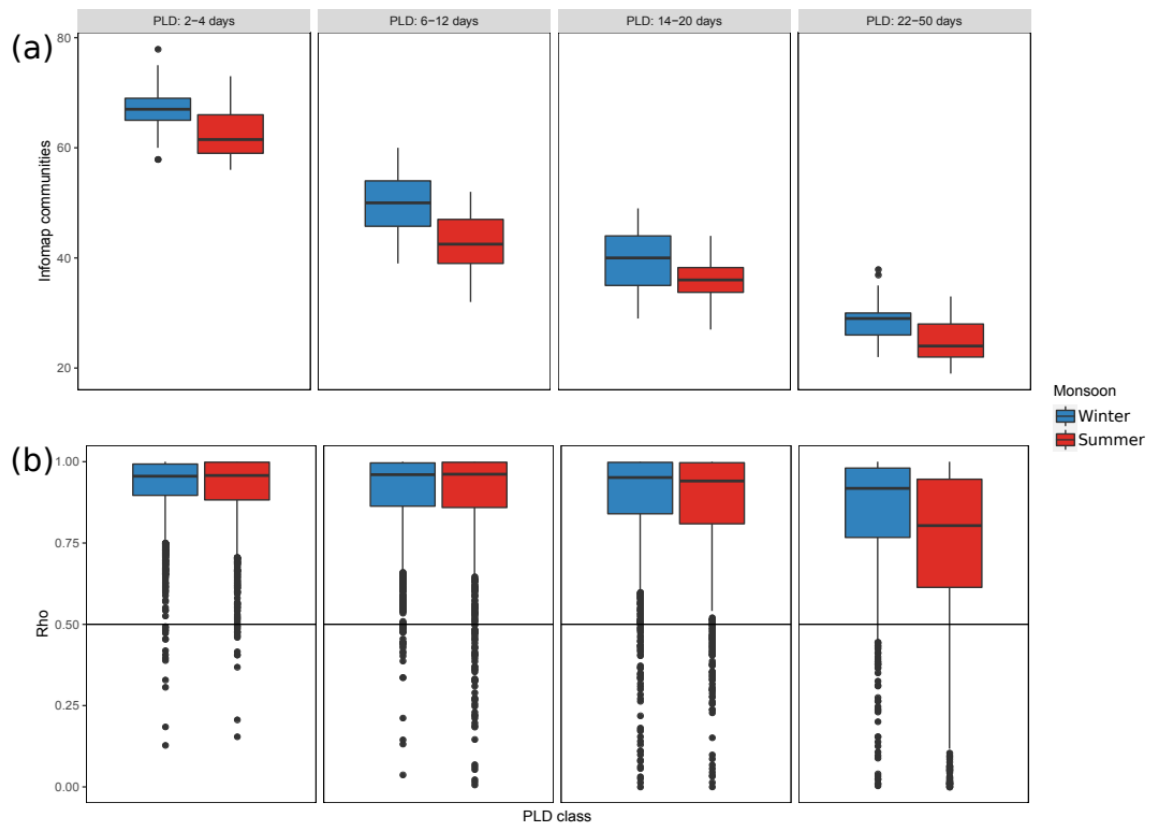
306

307 The location of community breaks varied with PLD, season and release period (indicated by  
308 the variation in the consistency of breaks within a PLD-class). However, a few locations  
309 frequently appeared as community breaks across release periods (>50% frequency), with  
310 some occurring persistently with a frequency greater than 90% (Figure 5). These community  
311 breaks were found along the north-west coast of mainland India (south of the Gulf of  
312 Khambhat 21°N, and Gulf of Kutch), Palk Strait (a narrow channel separating the Indian  
313 landmass from Sri Lanka) and north-east India, across both seasons (Figure 5). In the summer  
314 monsoon, a persistent community break appeared at the southern tip of India for all PLDs.  
315 Additional breaks also appeared along the west and east coast of India for PLD less than 20  
316 days, but were not consistent across season and PLD.

317

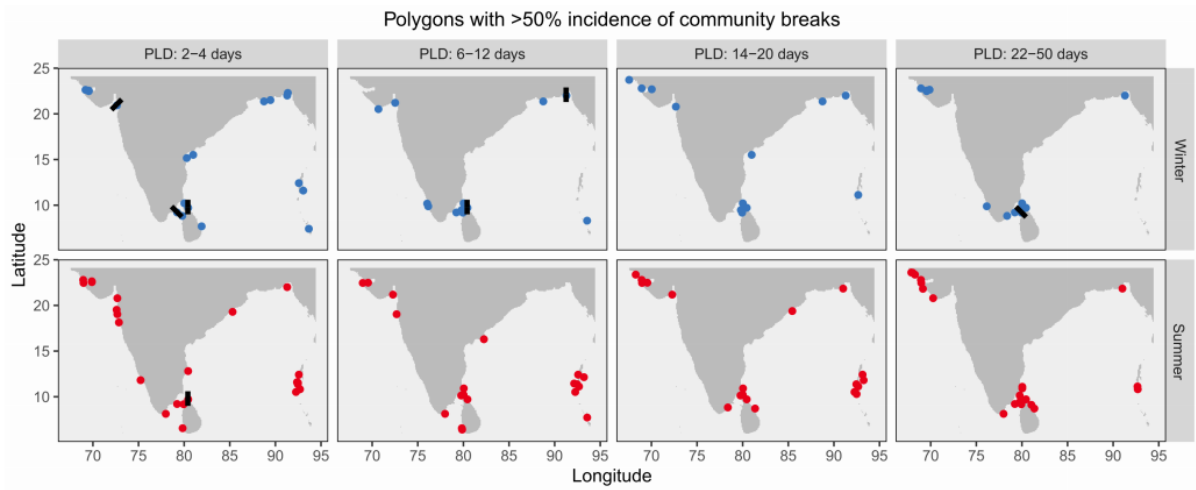
318 Based on PLD and season, the island groups varied in their connectivity with the coastal  
319 provinces along mainland India defined by the community breaks described above. In

320 general, median community similarity was greater at the larger PLD-class and during the  
321 summer monsoon. While Sri Lanka was well connected with most regions except the north-  
322 west coast, the Lakshadweep islands and the Nicobar islands were limited in their  
323 connectivity to the linear west coast and the Andaman islands respectively (Supplementary  
324 Information 6).



325

326 **Figure 4.** (a) Number of Infomap communities and (b) their coherence ratio.



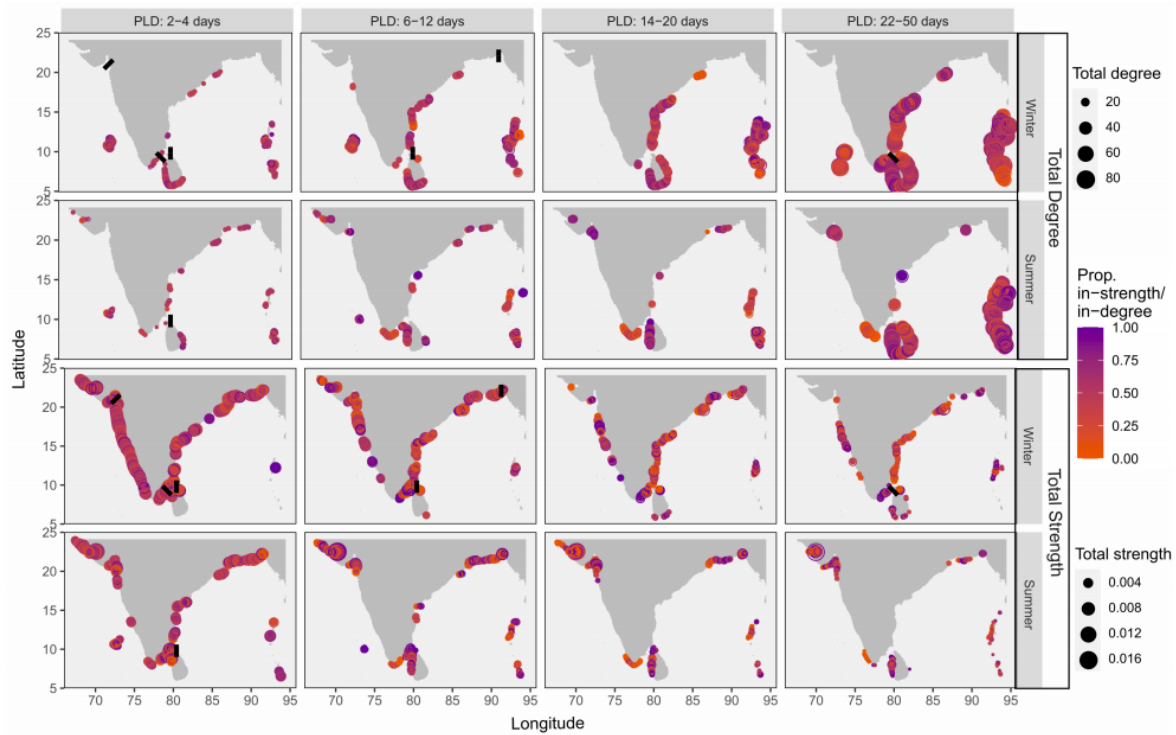
327

328 **Figure 5.** Distribution of Infomap community breaks. Blue and red circles indicate breaks  
 329 with frequency >50% across release periods for the winter and summer monsoon  
 330 respectively. Black bars indicate breaks with frequency >90% across release periods.

331 *Node descriptors*

332

333 As observed with connectance and the number of Infomap communities, node degree  
334 increased with PLD as a longer transport duration promoted variability in transport (Figure  
335 6). The increase in node degree was not uniform in the study region, and was observed to be  
336 higher in the east coast of India and the Lakshadweep islands during the winter monsoon,  
337 southern tip of India during the summer monsoon, and Sri Lanka and the Andaman and  
338 Nicobar islands during both the seasons (Figure 6). A consequence of transport over longer  
339 durations was the loss of particles from the coastal zone as observed from a decrease in the  
340 node strength in both seasons (Figure 6). However, in the winter monsoon, node strength  
341 showed lesser spatial variability and decreased more gradually with longer PLD as compared  
342 to the summer monsoon (Figure 6). The proportion of total node degree and strength  
343 contributed by incoming edges did not show stark large-scale spatial patterns, which may be  
344 associated with prominent source or sink populations.



345

346 **Figure 6.** Spatial distribution of total strength (sum of incoming and outgoing edge weights)  
 347 and degree (sum of number of incoming and outgoing edges). Nodes presented here have  
 348 strength/degree values greater than the median atleast 75% times across release periods in a  
 349 given PLD-class. The colour of a node reflects the magnitude of **proportion** in-  
 350 strength/degree, ranging from orange (source) to blue (sink). At each node, the size of the  
 351 filled circles represent the median and the concentric open circles represent the 75<sup>th</sup> quantile  
 352 of degree/strength. Infomap community breaks with >90% incidence are shown as black bars.

## 353 Discussion

354

355 This is the first broad-scale study to use ocean flow data and particle tracking models across a  
356 wide range of pelagic larval duration (PLD) and temporal scales to describe patterns of  
357 coastal connectivity along the Indian subcontinent and the adjacent island groups. We find  
358 that properties of connectivity networks exhibited large intra-seasonal and moderate inter-  
359 seasonal variability, but were comparable across years. *Though connectance was relatively*  
360 *low within the Indian coastline connectivity network (0.5 to 3.4%) as compared to other*  
361 *regions (4.8% to 25.8%) (Andrello et al., 2013; Agostini et al., 2015; Crochelet, et al., 2016),*  
362 *a PLD of 20 days was pivotal in ensuring significant transport farther than 2-5 km along the*  
363 *coastline, resulting in a few large well-connected coastal communities.*

364

### 365 *Connectivity provinces and biogeography*

366

367 Despite seasonal differences in the location of community breaks, particularly for PLD less  
368 20 days, four persistent disconnected provinces were identified along the mainland coast  
369 (Figure 8a). From west to east along the coastline of the Indian subcontinent, the first  
370 province extended across the Gulf of Khambhat and the coast of Gujarat (southern boundary at  
371 21°N), the second province was found along the west coast of India (~21°N to 8°N), the third  
372 province observed in the summer monsoon extended from the southern tip of India to the  
373 Palk strait (8-11°N, Gulf of Mannar, between Sri Lanka and mainland India) and the fourth  
374 province was observed along the east coast of India (~11°N up to 22°N). The island groups  
375 differed in their connectivity with these provinces, where Sri Lanka was well connected to

376 most regions, while the Lakshadweep and Nicobar islands were more isolated from the  
377 mainland connectivity provinces.

378

379 Three of the four coastal provinces delineated in our study remained stable across seasons  
380 despite the striking seasonal reversal of the upper ocean circulation along the Indian  
381 coastline. The extent of the observed provinces is congruent with two oceanographic features  
382 – the salinity front north of 20-21°N in the Arabian Sea (Luis & Kawamura, 2004) and the  
383 deviation in coastal circulation around Sri Lanka near the southern tip of the Indian coastline  
384 (Schott & McCreary, 2001).

385

386 Flow separation around 21°N in the northern Arabian Sea likely leads to the predicted  
387 connectivity break and the stability of a salinity front in this region, which is the southern  
388 limit of the Arabian Sea High Salinity Water Mass in the winter monsoon (Kumar & Prasad,  
389 1999). This salinity front is also associated with greater productivity in the water column as a  
390 result of upwelling (Madhupratap et al., 1996). While pelagic species distributions can be  
391 influenced by connectivity breaks, environmental differences or both, the composition of  
392 benthic invertebrates aligns more closely with the predicted connectivity province (Sivadas &  
393 Ingole, 2016; Figure 8b) in comparison to ecological units defined using climatological  
394 parameters (Sayre et al., 2017; Figure 8c). The present study encourages the incorporation of  
395 additional parameters that integrate ocean dynamics with climatology to delineate  
396 biogeographic units..

397

398 Despite some mismatch in the precise location of the predicted connectivity breaks and  
399 observed biogeographic boundaries, the connectivity provinces delineated in the north-west

400 coast and southern India overlap with divisions recognized using benthic and pelagic  
401 biogeography, supporting a relationship between ocean flow, environmental properties and  
402 species distributions (Spalding et al., 2007; Sivadas & Ingole, 2016, Figure 8c). Other  
403 biogeographic subdivisions that have been proposed along the east coast were recovered as  
404 community breaks for a specific subset of PLD-class and season (Figure 5 and Figure 8c),  
405 pointing to the importance of biotic filters of connectivity.

406

407 *Oceanographic drivers of connectivity*

408

409 Interestingly, though the monsoon is a key driver of the circulation around the Indian  
410 peninsula, its inter-annual variability, related to the El Niño–Southern Oscillation had a lower  
411 influence on all descriptors of coastal connectivity. In comparison, there was a larger effect of  
412 atmospheric intra-seasonal oscillations that result in short-lived upwelling/downwelling  
413 events along the Indian coastline (Varkey et al., 1996; Luis & Kawamura, 2004; Durand et  
414 al., 2009). When spawning time interacts with such intra-seasonal oscillations, dispersal  
415 descriptors can show intra-seasonal variability for PLDs shorter than the temporal scale of  
416 flow variability (Guizien et al., 2012). In the Indian Ocean, these atmospheric oscillations  
417 span over a wide range of time-scales ranging from a week to 60 days (Madden & Julian,  
418 1972; Fu et al., 2003), which likely explains why intra-seasonal variability was not averaged  
419 out across the PLD range of 2 to 50 days considered in the present study.

420

421 Studies from other ocean basins have found regional differences in the relative influence of  
422 intra-seasonal, inter-seasonal and inter-annual flow variability on connectivity patterns.  
423 Connectivity metrics are determined by geography more than seasonal and inter-annual

424 variability in circulation in the northern Indo-West Pacific (Pata & Yñiguez, 2019), while in  
425 Southern California, intra-seasonal variation alone contributes to half of the uncertainty in  
426 connectivity across temporal scales (Mitarai et al., 2009). In contrast, seasonal variation in  
427 circulation has a more significant influence on the structure of hydrodynamical provinces in  
428 the Mediterranean Sea (Rossi et al., 2014), and interacts with inter-annual variability in  
429 driving the spatial extent of connectivity along south-east Australia (Roughan et al., 2011).  
430 The absence of a strong seasonal influence in our study can be related to short-lived  
431 connectivity between a range of sites promoted by strong intra-seasonal flow variability  
432 leading to variation in connectivity breaks along shallow coastal regions, which has also been  
433 reported in other regions (Vaz et al., 2013; Rossi et al., 2014).

434

435 These results advocate for fine-tuning connectivity studies in the future to include a better  
436 description of short-lived atmospheric processes and to down-scale flow modelling within  
437 each of the provinces delineated in the present study.

438

439 *Genetic connectivity and future sampling effort*

440

441 Connectivity disruptions observed using genetic divergence among populations has only been  
442 tested in a few species along the Indian coastline. The extent of the observed genetic breaks  
443 broadly coincide with connectivity breaks predicted around the north-west coast, southern  
444 India and the Palk Strait (Figure 8b). However, many of these studies have low sampling  
445 effort along the coastline, which limits the accurate detection of genetic breaks and the ability  
446 to differentiate between isolation by distance and dispersal barriers in shaping population  
447 genetic structure (Audzijonyte & Vrijenhoek, 2010). Future population genetics studies using

448 a more continuous sampling strategy along the coastline will be necessary to evaluate the  
449 influence of ocean flow disruptions predicted here in shaping patterns of genetic connectivity.

450

451 Traits related to release timing and PLD act as biotic filters over connectivity patterns by  
452 determining the time-dependent ocean flow scenarios experienced by larvae. By combining  
453 information on spawning season and PLD range of the species of interest (Supplementary  
454 Information 3) with connectivity descriptors from the present study, it is possible to propose  
455 taxa-specific predictions of connectivity breaks, which could be empirically tested. For  
456 instance, in the case of taxa with likely summer spawning such as anthozoans (PLD < 7 days)  
457 and holothurians (PLD > 20 days), important connectivity breaks would be predicted to occur  
458 around the southern tip of India, Palk Strait, south-west Sri Lanka and ~20-21°N on the west  
459 coast of India. In contrast, likely winter spawners such as crustaceans (PLD < 20 days) and  
460 gastropods (PLD = 12-45 days), connectivity breaks would be predicted to occur around the  
461 Gulf of Khambat, Palk Strait and the north-east Indian coastline. For other taxonomic groups,  
462 which show a large variability in their spawning period (bivalves) or PLD (non-holothurian  
463 echinoderms), using species-specific traits to obtain predictions can help in guiding sampling  
464 effort for comparison with genetic estimates of connectivity (PLD and spawning information  
465 for benthic invertebrates from the Indian Ocean summarized in Figure S3.4, Supplementary  
466 Information 3).

467

468 However, large-scale transport simulations using neutrally buoyant particles with PLD and  
469 release period as the only biological parameters, can fail to predict taxa-specific connectivity  
470 breaks for various reasons. The transport of neutrally buoyant particles may considerably  
471 differ from that of buoyant or swimming larvae (Robins et al., 2013), especially in complex

472 flow scenarios (Condie & Condie, 2016) and in taxa with efficient larval swimmers (Condie  
473 et al. 1999). In addition, ocean flow simulations, with a coarse spatial resolution are  
474 inadequate to describe the fine-scale connectivity patterns in fragmented and spatially  
475 complex coastal habitats (Padrón et al. 2018; Frys et al., 2020). Finally, biotic filters acting  
476 pre- and post-transport (sensu Pineda et al. 2007), which are not accounted for in biophysical  
477 models, are likely to explain additional breaks at the level of demographic or genetic  
478 connectivity.

479

#### 480 *Implications for biodiversity conservation*

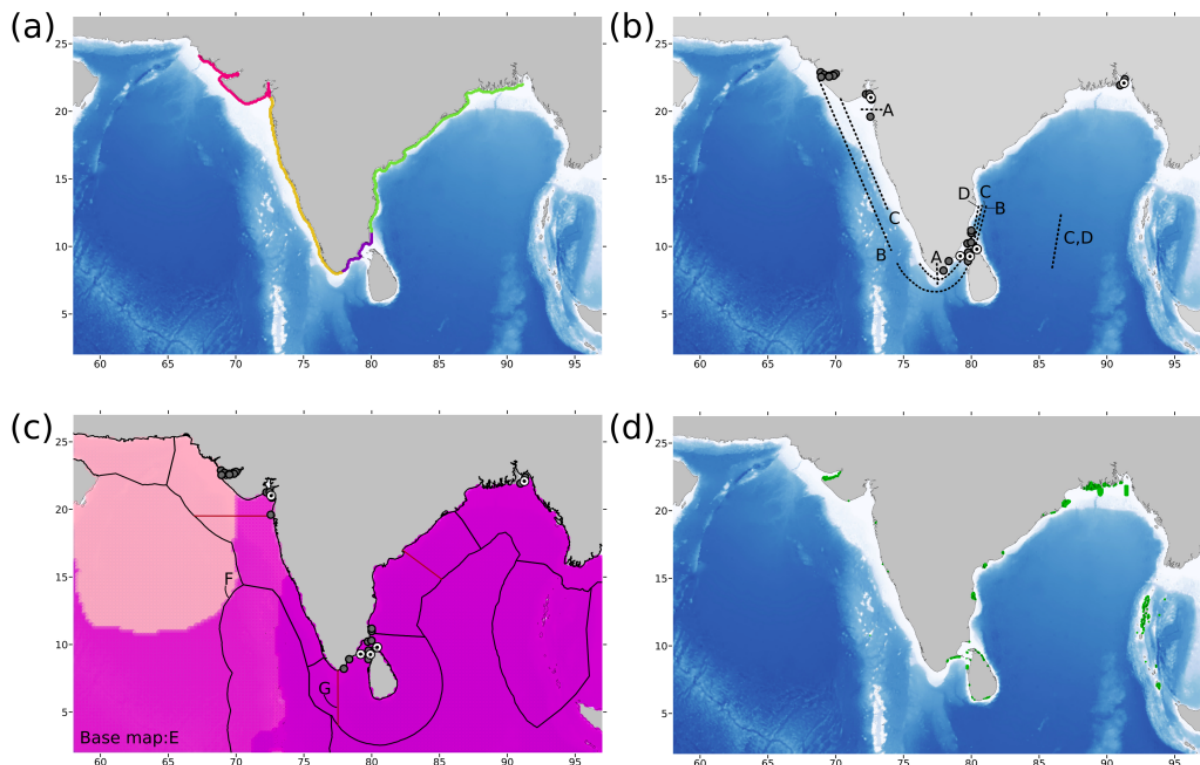
481

482 The community breaks identified from our study mark the scale and extent of metapopulation  
483 connectivity along the Indian coastline, and can be used to guide the management of marine  
484 biodiversity. Currently, Marine Protected Areas (MPAs) are located within each of the  
485 provinces delineated by our study, though large protected areas, including national parks, are  
486 missing along the linear west coast of India (Figure 8d). The identified connectivity provinces  
487 define the spatial extent within which high-resolution biophysical models can be developed to  
488 capture fine-scale population connectivity and source-sink dynamics within a  
489 metapopulation. This is especially important in evaluating the role of MPAs occurring in  
490 areas with recurrent connectivity breaks such as the Gulf of Mannar, Palk Strait, Andaman  
491 and Nicobar islands and the Gulf of Kutch. In these regions with complex coastal bathymetry,  
492 where connectivity breaks were detected at small spatial distances, spatially and temporally  
493 refined transport studies are key in accounting for the effect of fine-scale ocean features on  
494 flow connectivity (Briton et al. 2018, Guizien et al. 2012, 2014).

495

496 The wide extent of the predicted connectivity provinces also suggests the need for  
497 coordinated management of coastal biodiversity across regional jurisdictional, and  
498 transnational boundaries. Two of the Indian MPAs listed under the IUCN Transboundary  
499 Protected Area programme with Bangladesh and Sri Lanka, as well as MPAs and sites  
500 identified as Important Coastal and Marine Areas (Sivakumar et al., 2013) need to be  
501 evaluated for effectiveness of spatial and temporal connectivity in the future.

502



503

504 **Figure 8.** (a) Connectivity provinces predicted in the current study; (b) location of genetic  
 505 breaks in A. intertidal snails (Bharti, 2019), possible extent within which genetic breaks may  
 506 occur in B. a marine fish *Rachycentron canadum* (Divya et al., 2017), C. a shrimp *Penaeus*  
 507 *indicus* (Sajeela et al., 2019) and D. a mussel *Perna viridis* (Divya et al., 2020); (c)  
 508 classification corresponding to F. Ecological Marine Units (purple and pink) (Sayre et al.,  
 509 2017), E. Marine Ecoregions of the World (black outline) (Spalding et al., 2007), and G.  
 510 Ecoregion subdivisions from benthic community composition (red lines) (Sivadas & Ingole,  
 511 2016); (d) marine protected areas (wiiervis.nic.in). In sub-figures (b) and (c) community  
 512 breaks detected in this study are depicted using grey (>50% frequency) and concentric black  
 513 (>90% frequency) circles.

514 To conclude, the present study provides a coarse prediction of connectivity provinces valid in  
515 both monsoon regimes that fulfil a gap in marine biogeography studies from this region. Our  
516 results can guide the spatial scales at which future biophysical models should be set up.  
517 Based on the frequency of community breaks, we advocate for refining transport studies  
518 based on flow modelling and species habitat mapping at the appropriate resolution along the  
519 Gujarat coastline, around the southern tip of India and Sri Lanka, over two large areas  
520 extending along the western and eastern coasts of the Indian subcontinent, and within each of  
521 the island groups.

## 522 References

- 523 1 Amol, P., Shankar, D., Fernando, V., Mukherjee, A., Aparna, S. G., Fernandes, R.,  
524 Michael, G. S., Khalap, S. T., Satelkar, N. P., Agarvadekar, Y., Gaonkar, M. G., Tari,  
525 A. P., Kankonkar, A., & Vernekar, S. P. (2014). Observed intraseasonal and seasonal  
526 variability of the West India Coastal Current on the continental slope. *Journal of*  
527 *Earth System Science*, 123(5), 1045–1074. <https://doi.org/10.1007/s12040-014-0449-5>
- 528 2 Andrello, M., Mouillot, D., Beuvier, J., Albouy, C., Thuiller, W., & Manel, S. (2013).  
529 Low connectivity between Mediterranean marine protected areas: A biophysical  
530 modeling approach for the dusky grouper *Epinephelus marginatus*. *PLOS ONE*, 8(7),  
531 [e68564. https://doi.org/10.1371/journal.pone.0068564](https://doi.org/10.1371/journal.pone.0068564)
- 532 3 Audzijonyte, A., & Vrijenhoek, R. C. (2010). When gaps really are gaps: Statistical  
533 phylogeography of hydrothermal vent invertebrates. *Evolution; International Journal*  
534 *of Organic Evolution*, 64(8), 2369–2384. [https://doi.org/10.1111/j.1558-](https://doi.org/10.1111/j.1558-5646.2010.00987.x)  
535 [5646.2010.00987.x](https://doi.org/10.1111/j.1558-5646.2010.00987.x)
- 536 4 Baselga, A. (2017). Partitioning abundance-based multiple-site dissimilarity into  
537 components: Balanced variation in abundance and abundance gradients. *Methods in*  
538 *Ecology and Evolution*, 8(7), 799–808. <https://doi.org/10.1111/2041-210X.12693>
- 539 5 Baselga, A., & Orme, C. D. L. (2012). betapart: An R package for the study of beta  
540 diversity. *Methods in Ecology and Evolution*, 3(5), 808–812.  
541 <https://doi.org/10.1111/j.2041-210X.2012.00224.x>
- 542 6 Bharti, D. K. (2019). *Dispersal patterns and processes in littorinid snails along the*  
543 *Indian coastline*. Indian Institute of Science, Bangalore.
- 544 7 Bivand, R., & Rundel, C. (2020). *rgeos: Interface to Geometry Engine—Open Source*  
545 *(‘GEOS’)*. <https://cran.r-project.org/package=rgeos>

- 546 8 Bivand, R. S., Pebesma, E., & Gómez-Rubio, V. (2013). *Applied spatial data analysis*  
547 *with R* (2nd ed.). Springer-Verlag. <https://doi.org/10.1007/978-1-4614-7618-4>
- 548 9 Briton, F., Cortese, D., Duhaut, T., & Guizien, K. (2018). High-resolution modelling  
549 of ocean circulation can reveal retention spots important for biodiversity conservation.  
550 *Aquatic Conservation: Marine and Freshwater Ecosystems*, 28(4), 882–893.  
551 <https://doi.org/10.1002/aqc.2901>
- 552 10 Chassignet, E. P., Hurlburt, H. E., Smedstad, O. M., Halliwell, G. R., Hogan, P. J.,  
553 Wallcraft, A. J., Baraille, R., & Bleck, R. (2007). The HYCOM (HYbrid Coordinate  
554 Ocean Model) data assimilative system. *Journal of Marine Systems*, 65(1), 60–83.  
555 <https://doi.org/10.1016/j.jmarsys.2005.09.016>
- 556 11 Condie, S., Loneragan, N., & Die, D. (1999). Modelling the recruitment of tiger  
557 prawns *Penaeus esculentus* and *P. semisulcatus* to nursery grounds in the Gulf of  
558 Carpentaria, northern Australia: Implications for assessing stock-recruitment  
559 relationships. *Marine Ecology-Progress Series*, 178, 55–68.  
560 <https://doi.org/10.3354/meps178055>
- 561 12 Condie, S., & Condie, R. (2016). Retention of plankton within ocean eddies. *Global*  
562 *Ecology and Biogeography*, 25(10), 1264–1277. <https://doi.org/10.1111/geb.12485>
- 563 13 Crochelet, E., Roberts, J., Lagabrielle, E., Obura, D., Petit, M., & Chabanet, P. (2016).  
564 [A model-based assessment of reef larvae dispersal in the Western Indian Ocean](#)  
565 [reveals regional connectivity patterns—Potential implications for conservation](#)  
566 [policies. \*Regional Studies in Marine Science\*, 7, 159-167.](#)  
567 <https://doi.org/10.1016/j.rsma.2016.06.007>
- 568 14 Csardi, G., & Nepusz, T. (2006). The igraph software package for complex network  
569 research. *InterJournal, Complex Systems*, 1695(5), 1–9.

- 570 15 D'Agostini, A., Gherardi, D. F. M., & Pezzi, L. P. (2015). Connectivity of marine  
571 protected areas and its relation with total kinetic energy. *PLOS ONE*, *10*(10),  
572 e0139601. <https://doi.org/10.1371/journal.pone.0139601>
- 573 16 Di Franco, A., & Guidetti, P. (2011). Patterns of variability in early-life traits of fishes  
574 depend on spatial scale of analysis. *Biology Letters*, *7*(3), 454–456.  
575 <https://doi.org/10.1098/rsbl.2010.1149>
- 576 17 Divya, P. R., Linu, J., Mohitha, C., Kathirvelpandian, A., Manoj, P., Basheer, V. S., &  
577 Gopalakrishnan, A. (2017). Deciphering demographic history and fine-scale  
578 population structure of cobia, *Rachycentron canadum* (Pisces: Rachycentridae) using  
579 microsatellite and mitochondrial markers. *Marine Biodiversity*, *49*(1), 381–393.  
580 <https://doi.org/10.1007/s12526-017-0817-x>
- 581 18 Divya, P. R., Jency, P. M. E., Joy, L., Kathirvelpandian, A., Singh, R. K., & Basheer,  
582 V. S. (2020). Population connectivity and genetic structure of Asian green mussel,  
583 *Perna viridis* along Indian waters assessed using mitochondrial markers. *Molecular*  
584 *Biology Reports*, *47*(7), 5061–5072. <https://doi.org/10.1007/s11033-020-05575-4>
- 585 19 Dubois, M., Rossi, V., Ser-Giacomi, E., Arnaud-Haond, S., López, C., & Hernández-  
586 García, E. (2016). Linking basin-scale connectivity, oceanography and population  
587 dynamics for the conservation and management of marine ecosystems. *Global*  
588 *Ecology and Biogeography*, *25*(5), 503–515. <https://doi.org/10.1111/geb.12431>
- 589 20 Durand, F., Shankar, D., Birol, F., & Shenoi, S. S. C. (2009). Spatiotemporal structure  
590 of the East India Coastal Current from satellite altimetry. *Journal of Geophysical*  
591 *Research: Oceans*, *114*(2), 1–18. <https://doi.org/10.1029/2008JC004807>
- 592 21 Frys, C., Saint-Amand, A., Le Hénaff, M., Figueiredo, J., Kuba, A., Walker, B.,  
593 Lambrechts, J., Vallaeys, V., Vincent, D., & Hanert, E. (2020). Fine-scale coral

- 594 connectivity pathways in the Florida Reef Tract: Implications for conservation and  
595 restoration. *Frontiers in Marine Science*, 7. <https://doi.org/10.3389/fmars.2020.00312>
- 596 22 Fu, X., Wang, B., Li, T., & McCreary, J. P. (2003). Coupling between northward-  
597 propagating, intraseasonal oscillations and Sea Surface Temperature in the Indian  
598 Ocean. *Journal of the Atmospheric Sciences*, 60(15), 1733–1753.  
599 [https://doi.org/10.1175/1520-0469\(2003\)060<1733:CBNIOA>2.0.CO;2](https://doi.org/10.1175/1520-0469(2003)060<1733:CBNIOA>2.0.CO;2)
- 600 23 Gaonkar, C. A., S.V., S., George, G., V.M., A., Vethamony, P., & Anil, A. C. (2012).  
601 Numerical simulations of barnacle larval dispersion coupled with field observations  
602 on larval abundance, settlement and recruitment in a tropical monsoon influenced  
603 coastal marine environment. *Journal of Marine Systems*, 94, 218–231.  
604 <https://doi.org/10.1016/j.jmarsys.2011.12.002>
- 605 24 George, G., Vethamony, P., Sudheesh, K., & Babu, M. T. (2011). Fish larval transport  
606 in a macro-tidal regime: Gulf of Kachchh, west coast of India. *Fisheries Research*,  
607 110(1), 160–169. <https://doi.org/10.1016/j.fishres.2011.04.002>
- 608 25 George, M. S., Bertino, L., Johannessen, O. M., & Samuelsen, A. (2010). Validation  
609 of a hybrid coordinate ocean model for the Indian Ocean. *Journal of Operational*  
610 *Oceanography*, 3(2), 25–38. <https://doi.org/10.1080/1755876X.2010.11020115>
- 611 26 Guizien, K., Belharet, M., Marsaleix, P., & Guarini, J. M. (2012). Using larval  
612 dispersal simulations for marine protected area design: Application to the Gulf of  
613 Lions (northwest Mediterranean). *Limnology and Oceanography*, 57(4), 1099–1112.  
614 <https://doi.org/10.4319/lo.2012.57.4.1099>
- 615 27 Guizien, K., Belharet, M., Moritz, C., & Guarini, J. M. (2014). Vulnerability of  
616 marine benthic metapopulations: Implications of spatially structured connectivity for

- 617 conservation practice in the Gulf of Lions (NW Mediterranean Sea). *Diversity and*  
618 *Distributions*, 20(12), 1392–1402. <https://doi.org/10.1111/ddi.12254>
- 619 28 Halpern, B. S., & Warner, R. R. (2003). Matching marine reserve design to reserve  
620 objectives. *Proceedings. Biological Sciences*, 270(1527), 1871–1878.  
621 <https://doi.org/10.1098/rspb.2003.2405>
- 622 29 Hanski, I., & Gaggiotti, O. (2004). Metapopulation biology: Past, present, and future.  
623 In I. Hanski & O. E. Gaggiotti (Eds.), *Ecology, Genetics and Evolution of*  
624 *Metapopulations* (pp. 3–22). Academic Press. [https://doi.org/10.1016/B978-](https://doi.org/10.1016/B978-012323448-3/50003-9)  
625 [012323448-3/50003-9](https://doi.org/10.1016/B978-012323448-3/50003-9)
- 626 30 Hijmans, R. J. (2017). *raster: Geographic data analysis and modeling*. [https://cran.r-](https://cran.r-project.org/package=raster)  
627 [project.org/package=raster](https://cran.r-project.org/package=raster)
- 628 31 Hood, R. R., Beckley, L. E., & Wiggert, J. D. (2017). Biogeochemical and ecological  
629 impacts of boundary currents in the Indian Ocean. *Progress in Oceanography*, 156,  
630 290–325. <https://doi.org/10.1016/j.pocean.2017.04.011>
- 631 32 [Jacobi, M. N., André, C., Döös, K., & Jonsson, P. R.](#) (2012). Identification of  
632 subpopulations from connectivity matrices. *Ecography*, 35(11), 1004–1016.  
633 <https://doi.org/10.1111/j.1600-0587.2012.07281.x>
- 634 33 Joseph, S., Srinivasu, U., Vijay, P., Srinivasan, A., & Siva Reddy, S. (2018). *A report*  
635 *on implementation of operational Global and Indian Ocean HYCOM at INCOIS*  
636 [Technical report]. INCOIS. <http://moeseprints.incois.gov.in/id/eprint/4503>
- 637 34 Kumar, S. P., & Prasad, T. G. (1999). Formation and spreading of Arabian Sea high-  
638 salinity water mass. *Journal of Geophysical Research*, 104(C1), 1455–1464.  
639 <https://doi.org/10.1029/1998jc900022>

- 640 35 Levin, L. A. (2006). Recent progress in understanding larval dispersal: New directions  
641 and digressions. *Integrative and Comparative Biology*, 46(3), 282–297.  
642 <https://doi.org/10.1093/icb/icj024>
- 643 36 Luis, A. J., & Kawamura, H. (2004). Air-sea interaction, coastal circulation and  
644 primary production in the eastern Arabian Sea: A review. *Journal of Oceanography*,  
645 60(3), 205–218. <https://doi.org/10.1023/B:JOCE.0000038327.33559.34>
- 646 37 Madden, R. A., & Julian, P. R. (1972). Description of global-scale circulation cells in  
647 the tropics with a 40–50 day period. *Journal of Atmospheric Sciences*, 29(6), 1109–  
648 1123. [https://doi.org/10.1175/1520-0469\(1972\)029<1109:DOGSCC>2.0.CO;2](https://doi.org/10.1175/1520-0469(1972)029<1109:DOGSCC>2.0.CO;2)
- 649 38 Madhupratap, M., Prasanna Kumar, S., Bhattathiri, P. M. A., Dileep Kumar, M.,  
650 Raghukumar, S., Nair, K. K. C., & Ramaiah, N. (1996). Mechanism of the biological  
651 response to winter cooling in the northeastern Arabian Sea. *Nature*, 384(6609), 549–  
652 552. <https://doi.org/10.1038/384549a0>
- 653 39 Madhupratap, M., Gopalakrishnan, T. C., Haridas, P., & Nair, K. K. C. (2001).  
654 Mesozooplankton biomass, composition and distribution in the Arabian Sea during  
655 the Fall Intermonsoon: Implications of oxygen gradients. *Deep-Sea Research Part II:  
656 Topical Studies in Oceanography*, 48(6–7), 1345–1368.  
657 [https://doi.org/10.1016/S0967-0645\(00\)00142-9](https://doi.org/10.1016/S0967-0645(00)00142-9)
- 658 40 Mertens, L. E. A., Treml, E. A., & von der Heyden, S. (2018). Genetic and  
659 biophysical models help define marine conservation focus areas. *Frontiers in Marine  
660 Science*, 5. <https://doi.org/10.3389/fmars.2018.00268>
- 661 41 Mitarai, S., Siegel, D. A., Watson, J. R., Dong, C., & McWilliams, J. C. (2009).  
662 Quantifying connectivity in the coastal ocean with application to the Southern

- 663 California Bight. *Journal of Geophysical Research: Oceans*, 114(C10).  
664 <https://doi.org/10.1029/2008JC005166>
- 665 42 Mukherjee, A., Shankar, D., Fernando, V., Amol, P., Aparna, S. G., Fernandes, R.,  
666 Michael, G. S., Khalap, S. T., Satelkar, N. P., Agarvadekar, Y., Gaonkar, M. G., Tari,  
667 A. P., Kankonkar, A., & Vernekar, S. (2014). Observed seasonal and intraseasonal  
668 variability of the East India Coastal Current on the continental slope. *Journal of Earth  
669 System Science*, 123(6), 1197–1232. <https://doi.org/10.1007/s12040-014-0471-7>
- 670 43 North, E., Gallego, A., & Petitgas, P. (2009). Manual of recommended practices for  
671 modelling physical – biological interactions during fish early life. *ICES Cooperative  
672 Research Report*, 295.  
673 [http://www.crrc.unh.edu/mwg/b\\_physical\\_transport/manualrecommmendedpractices.  
674 pdf](http://www.crrc.unh.edu/mwg/b_physical_transport/manualrecommmendedpractices.pdf)
- 675 44 Padrón, M., Costantini, F., Baksay, S., Bramanti, L., & Guizien, K. (2018). Passive  
676 larval transport explains recent gene flow in a Mediterranean gorgonian. *Coral Reefs*,  
677 37(2), 495–506. <https://doi.org/10.1007/s00338-018-1674-1>
- 678 45 Paris, C. B., Helgers, J., van Sebille, E., & Srinivasan, A. (2013). Connectivity  
679 Modeling System: A probabilistic modeling tool for the multi-scale tracking of biotic  
680 and abiotic variability in the ocean. *Environmental Modelling and Software*, 42, 47–  
681 54. <https://doi.org/10.1016/j.envsoft.2012.12.006>
- 682 46 Partelow, S., Schlüter, A., von Wehrden, H., Jänig, M., & Senff, P. (2018). A  
683 sustainability agenda for tropical marine science. *Conservation Letters*, 11(1), 1–14.  
684 <https://doi.org/10.1111/conl.12351>

- 685 47 Pata, P. R., & Yñiguez, A. T. (2019). Larval connectivity patterns of the North Indo-  
686 West Pacific coral reefs. *PLOS ONE*, *14*(7), e0219913.  
687 <https://doi.org/10.1371/journal.pone.0219913>
- 688 48 Pebesma, E., & Bivand, R. (2005). *sp: Classes and methods for spatial data in R*.  
689 <https://cran.r-project.org/web/packages/sp/>
- 690 49 Pineda, J., Hare, J. A., & Sponaungle, S. (2007). Larval transport and dispersal in the  
691 coastal ocean and consequences for population connectivity. *Oceanography*, *20*(3),  
692 22–39. <https://doi.org/10.5670/oceanog.2007.27>
- 693 50 QGIS.org, 2021. QGIS Geographic Information System. QGIS Association.  
694 <http://www.qgis.org>
- 695 51 R Core Team. (2019). R: A language and environment for statistical computing. R  
696 Foundation for Statistical Computing, Vienna, Austria. <https://www.r-project.org/>
- 697 52 Robins, P. E., Neill, S. P., Giménez, L., Jenkins, S. R., & Malham, S. K. (2013).  
698 Physical and biological controls on larval dispersal and connectivity in a highly  
699 energetic shelf sea. *Limnology and Oceanography*, *58*(2), 505–524.  
700 <https://doi.org/10.4319/lo.2013.58.2.0505>
- 701 53 Rossi, V., Ser-Giacomi, E., López, C., & Hernández-García, E. (2014). Hydrodynamic  
702 provinces and oceanic connectivity from a transport network help designing marine  
703 reserves. *Geophysical Research Letters*, *41*(8), 2883–2891.  
704 <https://doi.org/10.1002/2014GL059540>
- 705 54 Rosvall, M., & Bergstrom, C. T. (2008). Maps of random walks on complex networks  
706 reveal community structure. *Proceedings of the National Academy of Sciences of the*  
707 *United States of America*, *105*(4), 1118–1123.  
708 <https://doi.org/10.1073/pnas.0706851105>

- 709 55 Roughan, M., Macdonald, H. S., Baird, M. E., & Glasby, T. M. (2011). Modelling  
710 coastal connectivity in a Western Boundary Current: Seasonal and inter-annual  
711 variability. *Deep Sea Research Part II: Topical Studies in Oceanography*, 58(5), 628–  
712 644. <https://doi.org/10.1016/j.dsr2.2010.06.004>
- 713 56 Roughgarden, J., Gaines, S., & Possingham, H. (1988). Recruitment dynamics in  
714 complex life cycles. *Science*, 241(4872), 1460–1466.  
715 <https://doi.org/10.1126/science.11538249>
- 716 57 Sajeela, K. A., Gopalakrishnan, A., Basheer, V. S., Mandal, A., Bineesh, K. K.,  
717 Grinson, G., & Gopakumar, S. D. (2019). New insights from nuclear and  
718 mitochondrial markers on the genetic diversity and structure of the Indian white  
719 shrimp *Fenneropenaeus indicus* among the marginal seas in the Indian Ocean.  
720 *Molecular Phylogenetics and Evolution*, 136, 53–64.  
721 <https://doi.org/10.1016/j.ympev.2019.04.007>
- 722 58 Sayre, R., Breyer, S., Butler, K., Van Graafeiland, K., Costello, M., Harris, P., Goodin,  
723 K., Guinotte, J., Basher, Z., Kavanaugh, M., Halpin, P., Monaco, M., Cressie, N.,  
724 Aniello, P., Frye, C., & Stephens, D. (2017). A three-dimensional mapping of the  
725 ocean based on environmental data. *Oceanography*, 30(1), 90–103.  
726 <https://doi.org/10.5670/oceanog.2017.116>
- 727 59 Schott, F. A., & McCreary, J. P. (2001). The monsoon circulation of the Indian Ocean.  
728 *Progress in Oceanography*, 51(1), 1–123. [https://doi.org/10.1016/S0079-](https://doi.org/10.1016/S0079-6611(01)00083-0)  
729 [6611\(01\)00083-0](https://doi.org/10.1016/S0079-6611(01)00083-0)
- 730 60 Schott, F. A., Xie, S.-P., & McCreary, J. P. (2009). Indian Ocean circulation and  
731 climate variability. *Reviews of Geophysics*, 47(1).  
732 <https://doi.org/10.1029/2007RG000245>

- 733 61 Shetye, S. R., & Gouveia, A. D. (1998). *Coastal circulation in the North Indian*  
734 *Ocean: Coastal segment (14,S-W)*. John Wiley and Sons, New York, USA.  
735 <http://drs.nio.org/drs/handle/2264/1966>
- 736 62 Sivadas, S. K., & Ingole, B. S. (2016). Biodiversity and biogeography pattern of  
737 benthic communities in the coastal basins of India. *Marine Biology Research*, 12(8),  
738 797–816. <https://doi.org/10.1080/17451000.2016.1203949>
- 739 63 Sivakumar, K., Mathur, V. K., & Pande, A. (2013). Coastal And marine protected  
740 areas in India: Challenges and way forward. In *ENVIS Bulletin: Wildlife & Protected*  
741 *Areas* (Vol. 15, pp. 292–298). Wildlife Institute of India.
- 742 64 Spalding, M. D., Fox, H. E., Allen, G. R., Davidson, N., Ferdaña, Z., Finlayson, M.,  
743 Halpern, B. S., Jorge, M. A., Lombana, A. L., Lourie, S. A., Martin, K. D., McManus,  
744 E., Molnar, J., Recchia, C. A., & Robertson, J. (2007). Marine ecoregions of the  
745 world: A bioregionalization of coastal and shelf areas. *Bioscience*, 57(7), 573–583.  
746 <https://doi.org/10.1641/B570707>
- 747 65 Swearer, S. E., Treml, E. A., & Shima, J. S. (2019). A review of biophysical models of  
748 marine larval dispersal. *Oceanography and Marine Biology : An Annual Review*, 57,  
749 325–356.
- 750 66 Treml, E. A., & Halpin, P. N. (2012). Marine population connectivity identifies  
751 ecological neighbors for conservation planning in the Coral Triangle. *Conservation*  
752 *Letters*, 5(6), 441–449. <https://doi.org/10.1111/j.1755-263X.2012.00260.x>
- 753 67 Varkey, M. J., Murty, V. S. N., & Suryanarayana, A. (1996). Physical oceanography of  
754 the Bay of Bengal and Andaman Sea. *Oceanography and Marine Biology: An Annual*  
755 *Review*, 34, 1–70.

- 756 68 Vaz, A. C., Richards, K. J., Jia, Y., & Paris, C. B. (2013). Mesoscale flow variability  
757 and its impact on connectivity for the island of Hawai`i. *Geophysical Research*  
758 *Letters*, 40, 332–337. <https://doi.org/10.1029/2012GL054519>
- 759 69 Vinayachandran, P. N., & Yamagata, T. (1998). Monsoon response of the sea around  
760 Sri Lanka: Generation of thermal domes and anticyclonic vortices. *Journal of*  
761 *Physical Oceanography*, 28(10), 1946–1960. [https://doi.org/10.1175/1520-](https://doi.org/10.1175/1520-0485(1998)028<1946:MRO TSA>2.0.CO;2)  
762 [0485\(1998\)028<1946:MRO TSA>2.0.CO;2](https://doi.org/10.1175/1520-0485(1998)028<1946:MRO TSA>2.0.CO;2)
- 763 70 Vinayachandran, P. N. (2009). Impact of physical processes on chlorophyll  
764 distribution in the Bay of Bengal. In *Indian Ocean Biogeochemical Processes and*  
765 *Ecological Variability* (pp. 71–86). American Geophysical Union (AGU).  
766 <https://doi.org/10.1029/2008GM000705>
- 767 71 Vinayachandran, P. N. M., Masumoto, Y., Roberts, M., Hugget, J., Halo, I.,  
768 Chatterjee, A., Amol, P., Gupta, G. V. M., Singh, A., Mukherjee, A., Prakash, S.,  
769 Beckley, L. E., Raes, E. J., & Hood, R. (2021). Reviews and syntheses: Physical and  
770 biogeochemical processes associated with upwelling in the Indian Ocean.  
771 *Biogeosciences Discussions*, 1–128. <https://doi.org/10.5194/bg-2020-486>  
772

773 **Acknowledgements**

774

775 This work was supported by the Department of Biotechnology, Government of India  
776 (BT/PR15704/AAQ/3/758/2015). Collaborative work was facilitated by an EMBO Short-  
777 Term Fellowship (STF 7321) awarded to DKB to visit the Laboratoire d'Ecogéochimie des  
778 Environnements Benthiques at Observatoire Océanologique de Banyuls Sur Mer (SU/CNRS),  
779 France. Research fellowship to DKB was awarded by the Council of Scientific and Industrial  
780 Research, Government of India (09/079(2450)/2011-EMR-I). DKB is grateful to Aarti  
781 Krishnamoorthy, Aditya Dharapuram and Lakshmi Prasad Natarajan for offering technical  
782 support for running the particle tracking simulations.